MINERALOGY AND GEOCHEMISTRY OF PALEOCENE ULTRAMAFIC- AND SEDIMENTARY-HOSTED TALC DEPOSITS IN THE SOUTHERN PART OF THE SIVAS BASIN, TURKEY

HÜSEYIN YALÇIN* AND ÖMER BOZKAYA

Department of Geological Engineering, Cumhuriyet University, TR-58140 Sivas, Turkey

Abstract—Talc deposits, located mainly in three areas of north-central Turkey, are present in the ophiolitic series of the Cretaceous and in siliciclastic rocks of the Paleocene. Talc deposits related to ophiolites are between tectonite and cumulate occurring as beds and/or lenses and $0.1-3$ cm thick fracture fillings within a 5 m brecciated zone with a vein-type bedding. Sedimentary-hosted talc beds and semi-rounded to angular talc grains ($0.1-2$ cm) range in thickness from 0.1 to 30 cm within marls and conglomerates. Talc veins form lenses (a few meters long) and spheroidal and/or ellipsoidal nodules ($1-10$ cm). Calcite, dolomite, serpentine and/or mixed-layered illite-smectite (I-S) minerals are encountered in the talc samples. Serpentine with positive U and Hf anomalies, and talc with positive Nb and Zr anomalies, and negative Ta and Ce anomalies are typically depleted in P and Ti, based on chondrite-normalized trace element patterns. The light rare earth element content of sedimentary-hosted talc with a negative Gd anomaly is richer than those of ultramafic-hosted talc with a negative anomaly for Eu as well as serpentine. Significantly, talc with a uniquely sedimentary origin tends to be the principal source of Nb, Hf, Zr, La, Ce, Pr and Nd with respect to serpentine. $\delta^{18}O$ and δD values for talc range from $+13.8$ to $+17.5‰$ and -60 to $-36‰$, and those of serpentine are $+9.4$ and $-88‰$, indicating supergene conditions for sedimentary-hosted talc and hypogene for ultramafic-hosted talc. When compared with seawater, $\delta^{18}O$ data indicate temperatures of 68ºC and $80-98$ºC for the sedimentary- and ultramafic-hosted talc formations, respectively, and 100ºC for serpentine, suggesting that talcification and serpentinization of ultramafic rocks both occurred at nearly the same time with various stages. All data show that the talc occurrences are divided into two types based on their mode of formation. The first corresponds to a serpentinization stage within the ophiolites. The others are the neoformation products of sedimentary deposition, diagenetic and post-diagenetic processes, respectively. Sedimentary-hosted talc also seems to have inherited trace element and isotopic compositions from the parent ultramafic rocks.

Key Words—Hydrous Phyllosilicates, Isotopes, Major Elements, Ophiolite, *REE*, SEM, Trace Elements, XRD.

INTRODUCTION

Talc is a relatively rare mineral with respect to other phyllosilicate minerals, yet it is the major constituent of economic deposits of soapstone or steatites which are used in many industrial applications such as ceramics, paint, paper, roofing, plastics, rubber and cosmetics. Talc mineralization occurs by various mechanisms within very different host rocks of different ages and geological environments. These include the retrograde metamorphism and metasomatism of silica-rich dolomites (Moine *et al.*, 1989; Anderson *et al.*, 1990; Schandl *et al.*, 2002), ultramafic rocks (Naldrett, 1966; Linder *et al.*, 1992; El-Sharkawy, 2000; Tornos and Spiro, 2000), the metamorphism of submarine hydrothermal rocks associated with massive sulfide deposits (Aggarwal and Nesbitt, 1984; Bjerkgard and Bjorlykke, 1996), hydrothermal systems and assemblages (Huston

et al., 1993; Hecht *et al.*, 1999), prograde metamorphism of Mg-rich silicates (Sandrone, 1993) and supergene formations in laterites (Noack *et al.*, 1986). In contrast to these, reports of talc occurrences due to diagenetic processes are less commonly encountered in the literature.

Talc deposits extending over $1-2$ km^2 are located 50 km south of Sivas in north-central Turkey, and within a northeast−southwest belt ~50 km long and 10 km wide (Figure 1). Various small open-pit mines in the region have been operated intermittently since the 1960s and have an estimated reserve of ~194,000 tons of talc (Önem, 2000). The mining geology of talc occurrences has been revealed through work by the General Directorate of Mineral Research and Exploration (MTA) in Turkey in recent years, and has not been fully described in the international literature. This study focuses on the formation, origin, paragenesis and chronostratigraphic distribution of talc and associated minerals, as well as their mineralogical and geochemical properties, and it provides new data for constructing a suitable genetic and/or exploration tool for the talc deposits on the ophiolitic suite and related sedimentary basins in Turkey.

* E-mail address of corresponding author:
yalcin@cumhuriyet.edu.tr

GEOLOGICAL FRAMEWORK AND STRATIGRAPHY

It is generally believed that the convergence of the African and Arabian plates with Eurasia, which led to the N−S shortening and thickening across Anatolia, began in the Middle Eocene and evolved into its present setting by the Middle Miocene (Şengör and Yılmaz, 1981). The collision was accompanied by obduction of the Tethyan oceanic crust onto the neighboring continental terrains, resulting in the emplacement of ophiolitic sequences. The Sivas Basin (Figure 1), one of several Central Anatolian Basins (Koçyigit, 1991; Görür *et al.*, 1998), is located between the Central Anatolian Crystalline Complex and the Tauride Belt that

developed mainly after the closure of the northern branch of Neotethys during Late Cretaceous and Eocene times (Şengör and Yılmaz, 1981). The Sivas Basin is a collision-related peripheral foreland basin (Görür *et al.*, 1998) that formed during the Paleocene (Poisson *et al.*, 1996; Kavak, 1998), and its evolution was completed by the Middle Miocene. The lacustrine and/or fluviatile intra-cratonic basins such as the Kangal and Kızılırmak basins (Guezou *et al.*, 1996) formed in the Sivas Basin as part of the neotectonic regime in the late Miocene to late Pliocene (*e.g.* Şengör, 1979; Koçyigit, 1991; Poisson *et al.*, 1996; Görür *et al.*, 1998).

The Sivas talc deposits commonly occur within ultramafic and siliciclastic rocks which were deposited on the northern slopes of the northeast−southwest-
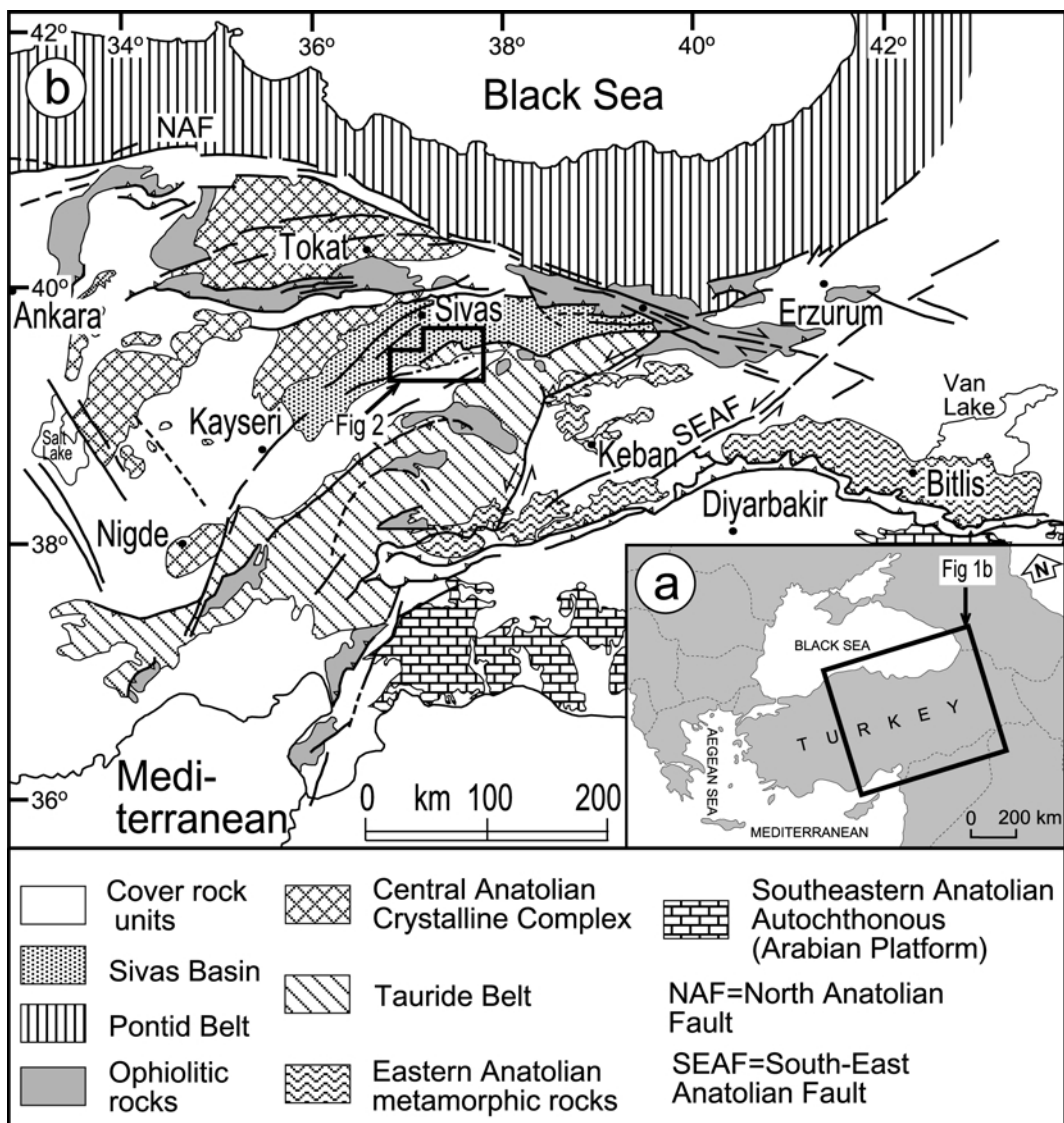

Figure 1. (a) Location map of Turkey and surrounding countries; (b) setting of the Sivas Basin in the regional geology (simplified and changed after Bingöl, 1989).

trending ophiolitic series (Figure 2). The key stratigraphic-tectonic features and geological mapping of the region were described by previous workers (Kurtman, 1973; Yılmaz *et al.*, 1989; Gökten, 1993; Poisson *et al.*, 1996; Kavak, 1998). The chronostratigraphic sequences suggested for the Sivas talc deposits by earlier investigators are as follows: the Çataldag limestone of late Jurassic–early Cretaceous age (Inan *et al.*, 1993), the Divrigi ophiolitic complex of late Cretaceous age (Tunç *et al.*, 1991) and the Tecer formation of late Cretaceous-early Paleocene age (Inan and Inan, 1990) form the basement of the Sivas Basin. The ophiolitic series consists mainly of serpentinized ultramafics such as dunite and orthopyroxenite, and igneous rocks such as uralitic gabbro, diorite and andesitic basalt. The Tecer formation consists of alternating massive, thick-bedded and blackish gray limestone-dolomitic limestone-dolomite (Yalçın and Inan, 1992).

The Yagmurluseki formation (Meşhur and Aziz, 1980) of Paleocene age, which is represented by red-colored and irregularly-bedded siliciclastic rocks such as conglomerates with ultramafic fragments, sandstones, siltstones, claystones and marls, and the Tecer formation, are locally transitional (Kavak, 1998).

Units of Eocene age in the marine facies are observed as volcanogenic formations. Of these, the Kaleköy formation (Gökten, 1983) includes green-colored and medium−thick-bedded pyroclastic rocks intercalated with basaltic andesite. The Bozbel formation (Kurtman, 1973) alternates with gray volcanic sandstone-shale-limestone and is intercalated with gypsum laminations and lenses at the top.

Oligocene marine units are the Selimiye formation (Kurtman, 1973) which alternates between light purple to red, and green sandstone-marl, the Hafik formation (Kurtman, 1973) with white massive gypsum intercalated with brown-red claystone-sandstone, and finally the Karayün formation (Cater *et al.*, 1991) with red sandstone-conglomerate alternations with marl intercalations.

The Karacaören formation of late Oligocene–early Miocene age (Kurtman, 1973) consists of alternating green claystone/marl-gypsum-sandstone and limestone at the base and calcarenite and reefal limestones at the top.

The late Miocene-Pliocene Incesu formation (Yılmaz, 1983) occurs in a continental facies covering gray, weakly-cemented conglomerate-sandstone with limestone and marl. The stratigraphic sequence in the region ends with Yamadagi volcanic rocks representing collision-zone magmatism (Yalçın *et al.*, 1998).

TALC DEPOSITS

Ultramafic-hosted talc mineralization in the Divrigi ophiolitic complex at Yenikervansaray, and sedimentary-hosted talc occurrences in the Yagmurluseki formation at Yagmurluseki and Kurtlukaya are represented in three stratigraphic columns (Figure 3).

In all deposits, the color of talc ranges from white to green, but clayey talc can be reddish. Individual grains are observed as anhedral crystals and as clusters of subparallel crystals. Soapstone-type talc has an appearance of slick and horn-like thin rods and firm fibrous aggregates.
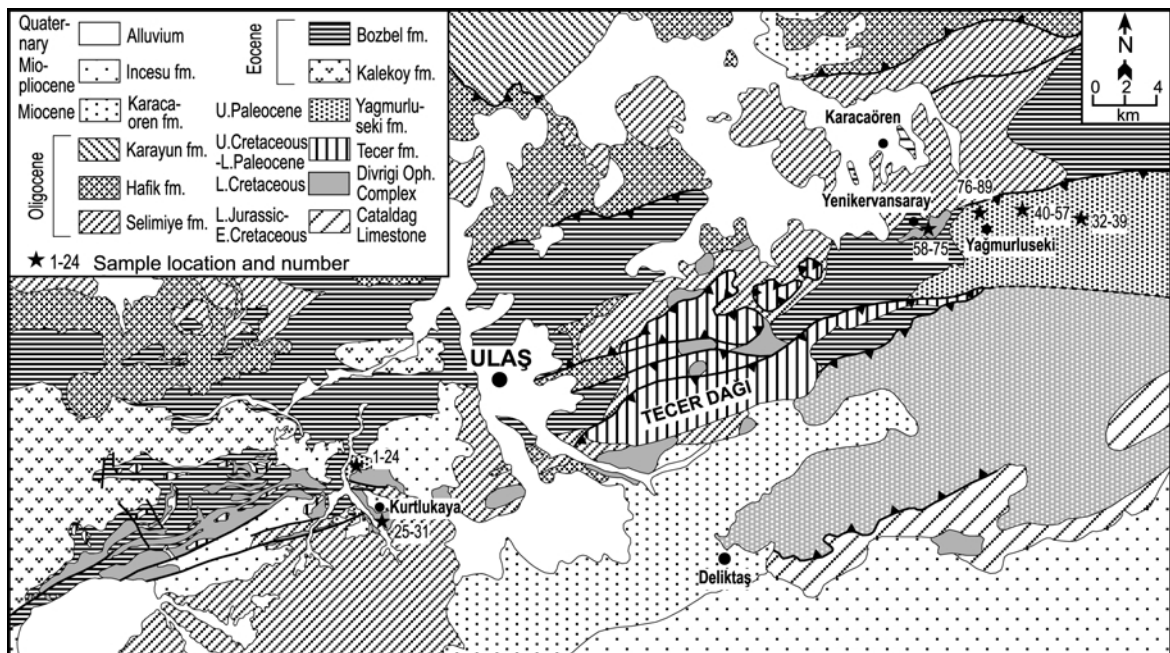

Figure 2. Geological map of the southern part of the Sivas Basin (prepared after Yılmaz *et al.*, 1989; Poisson *et al.*, 1996; Kavak, 1998; Gökten, 1993).
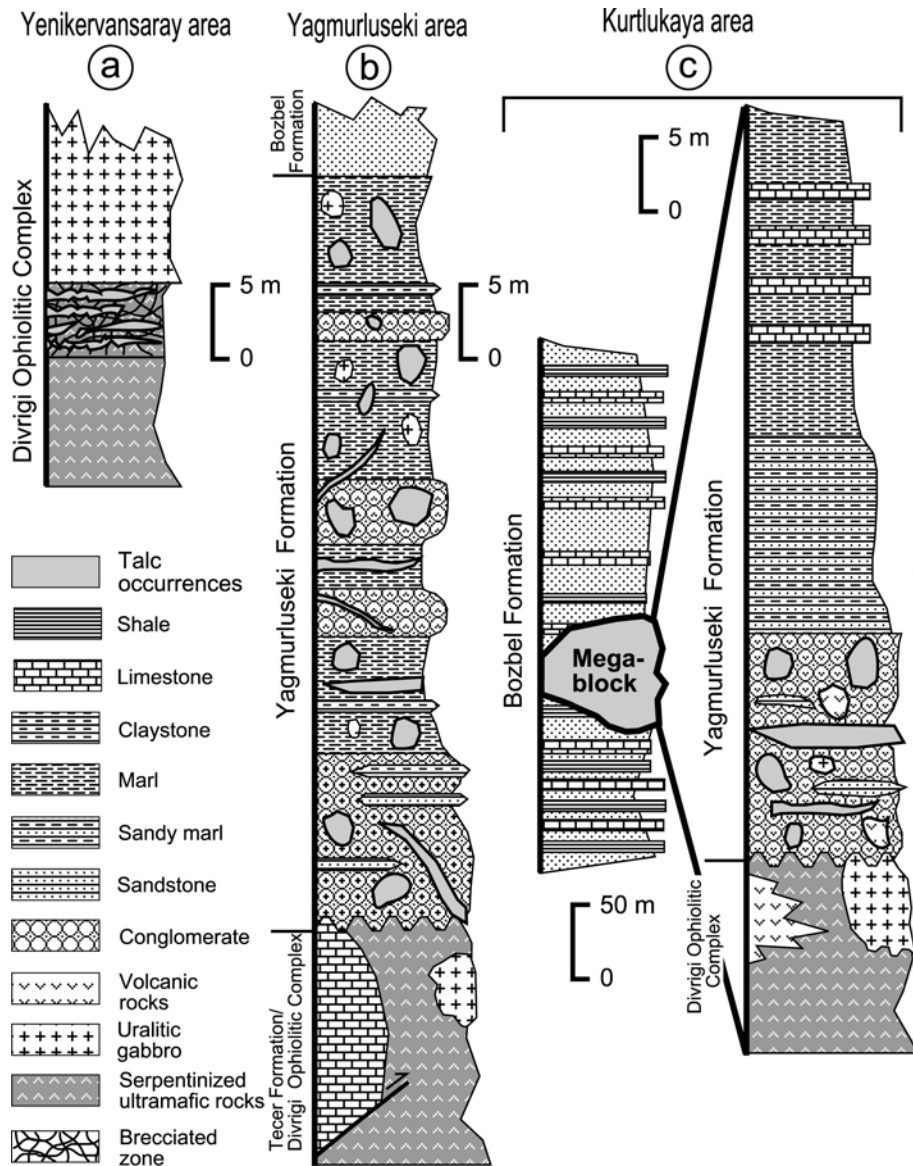
Figure 3. Generalized stratigraphic columns of the region, indicating of the locations of talc-bearing units.

Ultramafic-hosted talc occurrences

The deposits in the Yenikervansaray area are located between tectonite and cumulate of the ophiolitic sequence, and occur along a roughly EW/45°SE-trending main thrust fault. Tectonites are dark blackish-green, mesh-structured and completely serpentinized dunites including very thin (0.5−1 mm) talc-filled fractures, whereas the cumulates are represented by green-colored uralitic gabbros. Talc ores occur in vein-type bedding within a brecciated and crushed zone nearly 5 m thick and 200 m long (Figure 3a). Talc is found in bands, layers and/or lenses and fracture fillings (1 mm−3 cm) within the serpentinites. Talc and serpentinite levels alternate in the alteration zone.

Sedimentary-hosted talc occurrences

Talc beds in the Yagmurluseki area range from 1 mm to 30 cm thick within the siliciclastic rocks (Figure 3b) and have a general trend of EW/45−90°S, which is parallel to the same thrust lines. Talc veins form layers a few meters thick and lense-shaped bodies in some places (Figure 4a). Talc occurrences are also encountered as very irregular geometries that cross-cut the siliciclastic bedding with an obvious syn-sedimentary tectonic control. The larger (up to 10−20 cm) nodules are formed by joining spherical and/or ellipsoidal nodules of 1−2 cm in diameter (Figure 4b). In addition, the angular nodules 1 mm−10 cm in size were identified as microcrystalline grains within the claystone/marls. Red,
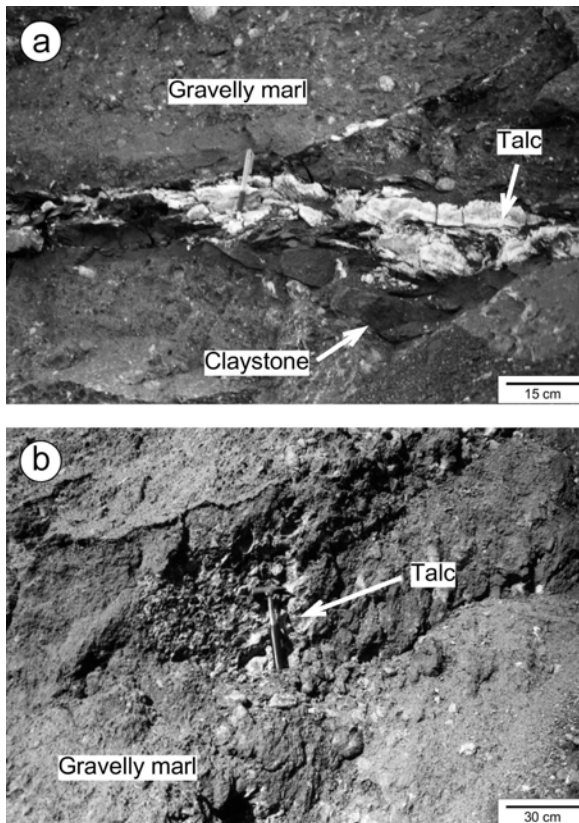
Figure 4. Talc occurrences from the Yagmurluseki area in the Sivas Basin: (a) layered and lens-shaped talc within thin claystones surrounded by the coarse-grained siliciclastic rocks; (b) nodular talc within the gravelly marl.

MATERIAL AND METHODS

A total of 89 samples was taken from units including talc mostly along measured sections. To confirm the mineralogical and chemical compositions of rock and minerals, the following techniques were used.

X-ray diffraction (XRD) patterns were recorded using a Rigaku DMAX IIIC model diffractometer operated at 35 kV and 15 mA with CuKα radiation, slits (divergence = 1°, scatter = 1°, receiving = 0.15 mm, receiving-monochromator = 0.30 mm) and scan speed of 2°2θ/min at the Laboratories of the Geological Engineering Department at Sivas Cumhuriyet University, Turkey. Samples were first washed in order to clean the surface, and then dried at room temperature and crushed and ground using a mortar and pestle. The acidified powders were washed repeatedly in distilled water until deflocculation occurred, using Calgon where necessary. The <2 μm fractions were separated by gravity settling, and oriented clay mounts were prepared by centrifugation with a Heraeus Sepatech Varifuge 3.2S on glass slides. Clay minerals were examined from 2−30°2θ in the air-dried state, after ethylene glycol solvation at 60°C for 16 h and after heating at 490°C for 4 h. The treated samples were run from 2 to 30°2θ, at a scan speed of 1°2θ/min and a step-scan 0.04°2θ.

Semi-quantitative percentages of both rock-forming minerals and clay fractions were calculated by means of mineral intensity factors based on the external standard method of Brindley (1980). The d values for the 211 and 101 reflections of quartz (59.982°2θ, d = 1.541 Å; 26.644°2θ, d = 3.343 Å) were taken as references for the measurements of d values of phyllosilicate minerals.

A polished surface of natural rock as thin slices and randomly oriented powder samples were prepared for identification of talc polytypes in the range 5−65°2θ. Powder methods were preferred because the peaks in natural samples have relatively low intensities. Egyptian talc samples obtained from a private company were added to this study for comparison.

Samples were coated with Au and scanning electron microscopy (SEM) images were obtained using a JEOL JSM-840A instrument at the Laboratories of the Turkish Petroleum Corporation, Turkey. The semi-quantitative micro-analysis of minerals was performed by energy dispersive spectrometry (EDS) with a JSM 6400 model equipped with a SEM and operated at an accelerating voltage of 20 kV.

The major element analyses of three mineral samples (ST-16, ST-29 and ST-74) were carried out using a Rigaku 3270 model X-ray fluorescence (XRF) spectrometer at Cumhuriyet University in Sivas. USGS (Flanagan, 1976), CRPG, GIT-IWG and ANRT (Govindaraju, 1989) rock standards were employed to calibrate and determine chemical concentrations. The estimated accuracy is ±2% for major oxides (SiO_2, TiO_2, Al_2O_3, ΣFe_2O_3, MnO, MgO, CaO, Na_2O, K_2O and P_2O_5).

coarse-grained siliciclastic rocks are found in the lower and upper parts of talc occurrences and consist of granules with serpentinite, gabbro and volcanic rock fragments. The pebbles with angular and subrounded forms reach up to 10 cm in size. The matrix of conglomerates varies from clay to sand having the same composition as the grains. White altered gabbro fragments are macroscopically similar to serpentinites, apart from the lack of talcification. The same types of pebbles are rarely identified within the claystones and talc bodies.

An ~3 m thick talc-rich zone with a N60°E/40°NW-trend in the Kurtlukaya area is located between green conglomerates with serpentinite and volcanic fragments at the bottom, and sandy marls at the top (Figure 3c). From sub-rounded to angular, talc grains, 1 mm−2 cm in size, have a brecciated appearance in the clayey matrix. Talc occurrences in this area are early Paleocene (Danian) in age based on fossil descriptions such as *Subbotina pseudobulloides* (PLUMMER) and *Globigerinidae* in the biomicrites. Although this location was mapped as Eocene by Yılmaz *et al.* (1989), Paleocene rocks are now known to occur as thin bands in the marginal facies of basins near ophiolites and/or megablocks within Eocene units.

Loss on ignition (LOI) of the samples reflects the total water and volatiles content as a weight percentage lost on heating at 1000°C for 16 h after drying at 110°C. The contents of major and some trace elements and rare-earth elements (*REE*) of other samples were analyzed with fusion inductively coupled plasma (ICP) and fusion inductively coupled plasma-mass spectrometry (ICP-MS) at Activation Laboratories Ltd., Canada. Major and trace elements were analyzed by the ICP and ICP-MS methods on the extracted pure talc and lizardite fractions. The most aggressive fusion technique employs a lithium metaborate/tetraborate fusion which ensures that the entire sample is dissolved. The resulting molten bead is rapidly digested in a weak nitric acid solution. O-H isotope data were measured on talc and lizardite minerals using thermal ionization mass spectrometry (TIMS).

PETROGRAPHY

Optical microscopy

Three types of serpentinite textures were determined on the basis of the classification of Wicks and Whittaker (1977) and Wicks and Plant (1979). Of these, the textures of the protolith are preserved in the pseudomorphic texture and represented by mesh cells in the ultramafics (Figure 5a), whereas it does not exist in the non-pseudomorphic texture. The other is a transitional texture in which only some features can be observed. The high degree of serpentinization of the ultramafic rocks makes it difficult to identify the primary minerals, but the pseudomorphs and relict minerals demonstrate that the primary minerals were predominantly olivine with lesser amounts of orthopyroxene and opaque minerals such as black magnetite and brown chromite. Clinopyroxene lamellae occur in enstatites and are serpentinized and form bastite. The hourglass texture can be distinguished in the serpentines. In addition, ribbon-like serpentine is found within the small veins, filling fractures and fractures. Relict olivine cannot be easily identified in the serpentinite although typical mesh texture is preserved.

The relict mesh texture in serpentinite indicates that talc crystallized after serpentine (Figure 5b). Talc with curved fibers and/or grains and serpentines with platy texture can be differentiated from crystal forms (Figure 5c−d). Fibrous and granular talc transitions corresponding to different formation stages and/or mechanisms are also recognized in talc samples with calcite (Figure 5e). Subhedral to euhedral dolomite with trigonal symmetry and calcite, as well as serpentine relics, are present within the fine-grained talc-altered serpentinites (Figure 5f).

Gabbros include uralitic hornblende and tremolite/actinolite, partly serpentinized and chloritized pyroxene and intensely argillized/sericitized plagioclase. Calcite, quartz and/or talc minerals can be also encountered within the fractures of some samples.

Felsic and mafic minerals as well as the matrix are completely converted to clay minerals in the vitrophyric-porphyric-textured volcanic rocks. Plagioclase, amphibole and pyroxene relics are identified in the basaltic andesite.

Scanning electron microscopy

In the ultramafic-hosted talcified serpentinites, lizardite 'bunches' have a vein-like appearance surrounded by talc blades (Figure 6a). Individual lizardite fibers parallel to each other are typically 20 μm long and ~1 μm in diameter (Figure 6b). Blade-shaped talc crystals range in size from 5 to 15 μm and have irregular edges that form rose-like aggregates in some places (Figure 6c). Analysis by EDS revealed them to be composed entirely of Si (58.757 wt.%), Mg (34.156 wt.%) and Fe (7.087 wt.%). The intergrown lizardite fibers and talc blades can also be seen (Figure 6d).

In the sedimentary-hosted talcified serpentinites, euhedral dolomite crystals, 12 μm in size, are present in trace quantities which developed within the pores of the rock (Figure 7a). Talc occurs as extremely fine-grained, thin flaky or smectite-like crystals on the surface of the matrix (Figure 7b). They appear as interlocking foliated masses of subhedral to equant flakes with a 'cornflake'-like texture. The semi-quantitative EDS analysis of this X-ray amorphous material showed that Si (56.729 wt.%), Mg (11.470 wt.%) and Fe (30.030 wt.%) are the only major constituents, with minor amounts of Ca (1.771 wt.%) also detected, *i.e.* similar in composition to serpentine. In the same sample with mesh texture, lizardite fibers were overgrown on the edges of meshes, whereas flaky talc was developed in the matrix rich in serpentine-like material (Figure 7c).

X-RAY MINERALOGY

The XRD patterns of representative samples bearing talc and serpentine assemblages are presented in Figures 8 and 9.

In the ulramafic-hosted talc occurrences in the Yenikervansaray area, talc and phyllosilicate are the main minerals. Feldspar, hornblende and phyllosilicate in the uralitized gabbros (Figure 8a) and feldspar, pyroxene, phyllosilicate and calcite in the altered andesitic basalts (Figure 8b) are also present. Calcite ranging from 4 to 11% in some samples of the talcified serpentines, and trace amount of dolomite (<2%) in one sample, were also detected (Figure 8c). Serpentine minerals associated with a negligible amount of talc are rare in the talc-unaltered serpentinites. The wide variety of phyllosilicate associations in mafic rocks is described as follows: illite + chlorite + mixed-layered chlorite-smectite (C-S) and smectite + illite + chlorite in the uralitized gabbros, and smectite + illite + chlorite + C-S in the diorites. An assemblage of talc + serpentine as
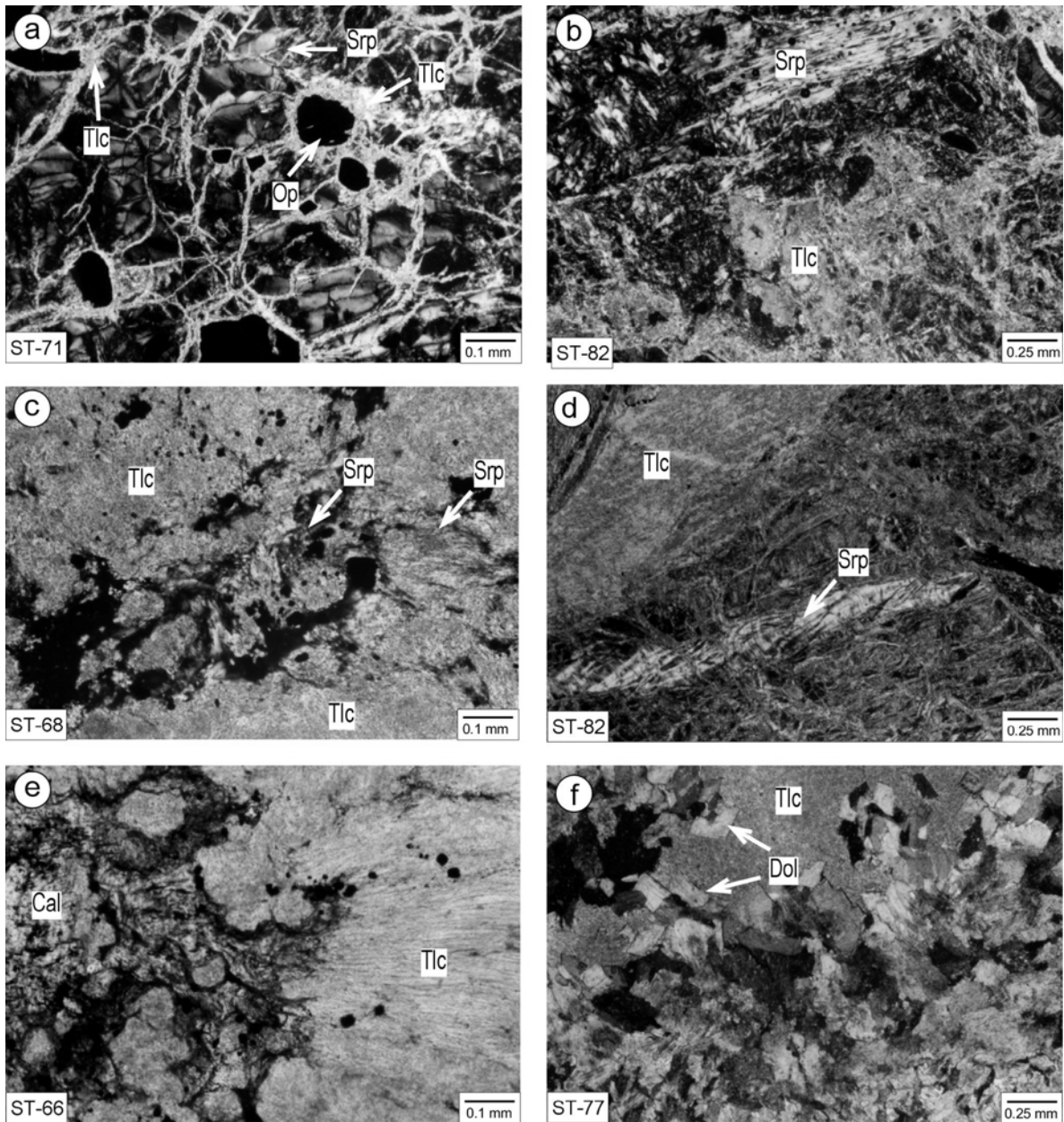
Figure 5. Optical micrographs of serpentinites and talcified serpentinites under crossed polars (a,e: Yenikervansaray area, b−d,f: Yagmurluseki area). (a) Hourglass-textured lizardites and common opaque minerals in the mesh-textured serpentinites, and brecciated talc filling cracks (Tlc = talc, Srp = serpentine, Op = opaque mineral). (b) Relationships between the granular talc and platy serpentine relics in the talcified serpentinites. (c) Fibrous talc and platy serpentine relics in the talcified serpentinites. (d) Fibrous talc transition to curved platy serpentine relics in the talcified serpentinites. (e) Granular and fibrous talc in the talcified serpentinites with subhedral calcites (Cal = calcite). (f) Fine-grained talc and euhedral dolomites in the talcified serpentinites (Dol = dolomite).

well as pure talc are common in the talc-altered serpentinites (Figure 9a−b).

Sedimentary rocks in the Yagmurluseki area contain quartz, calcite, dolomite and phyllosilicates (Figure 8d) such as smectite, chlorite, serpentine, talc, I-S and C-S. Uralitic gabbro pebbles within the siliciclastic rocks are formed of only chlorite or chlorite plus a small amount of illite (<10%). The altered volcanic fragments in the epiclastic rocks generally produce clay minerals and sometimes dolomite. Clay minerals are represented by chlorite + illite + C-S + smectite ± talc, serpentine + I-S + smectite, and chlorite + illite. Talc samples commonly have monomineralic phases, but small amounts of serpentine and dolomite are observed, and
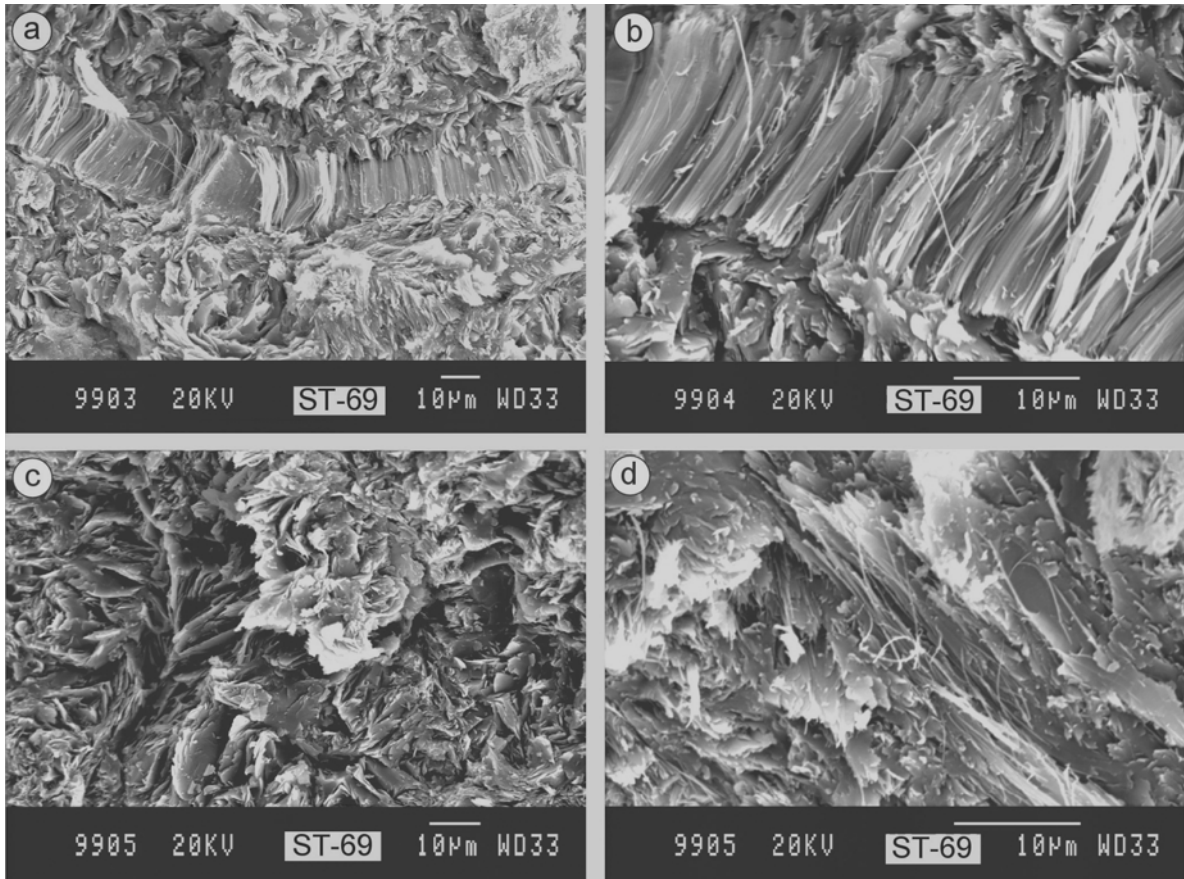
Figure 6. SEM images of ultramafic-hosted talcified serpentinites: (a) relationship between fibrous lizardite and platy talc; (b) close occurrence of lizardites with separable fibers; (c) rose-like talc aggregates with bladed shapes; (d) intergrowth of lizardite fibers and talc blades.

I-S and/or chlorite are rarely found in talc (Figure 9c). The interstratification is random and rich in illite. The illite content in I-S is estimated at 55% based on the method of Moore and Reynolds (1997).

Sedimentary-hosted rocks in the Kurtlukaya area contain quartz, feldspar, calcite, dolomite and phyllosilicates, in order of abundance (Figure 8e–f). The most common phyllosilicate minerals are serpentine and I-S in the marls. In addition to these, smectite, illite, C-S and lesser talc are identified in the clayey rocks. Serpentinite fragments are formed almost entirely of serpentine (Figure 9d). Talc and I-S (<10%) only occur in small quantities in the serpentinite (Figure 9e). Volcanic gravel is composed of chlorite or illite, chlorite, C-S, talc and smectite, depending on the degree of alteration. Chlorite has a series of basal diffraction peaks with the 001 reflection weaker than 002, indicating that it is Fe-rich (Figure 9f). Talc ores are characterized by predominantly pure talc minerals associated with calcite, with serpentine and I-S found locally in minor concentrations (<5%).

The XRD powder patterns allow us to classify the sedimentary- (Figure 10a) and ultramafic-hosted (Figure 10b) talc as polytypes of both two-layer monoclinic ($2M_A$) and one-layer triclinic ($1A_A$) based on d_{hkl} reflections determined by Wiewiora *et al.* (1997). The Sivas talc which includes mixed structures is also different from the Egyptian (Figure 10c) and Pueblo de Lillo (Spain) deposits in having a $1A_A$ polytype.

GEOCHEMISTRY

Major and trace elements

Chemical compositions for the representative phyllosilicates such as talc and serpentine (<2 μm) are given in Tables 1 and 2, and their structural formulae are evaluated on the basis of 11 and 7 oxygen atoms for talc and serpentine, respectively.

Silica, MgO and H_2O are the essential components of talc. Green talc derived from serpentinite gravels and pebbles within the siliciclastic rocks is relatively rich in Fe_2O_3 and poor in MgO, compared with talc from serpentinized tectonites. However, the white talc originating in ultramafic rocks and deposited in deeper facies, far from the ophiolitic belts, is partly richer in Mg.
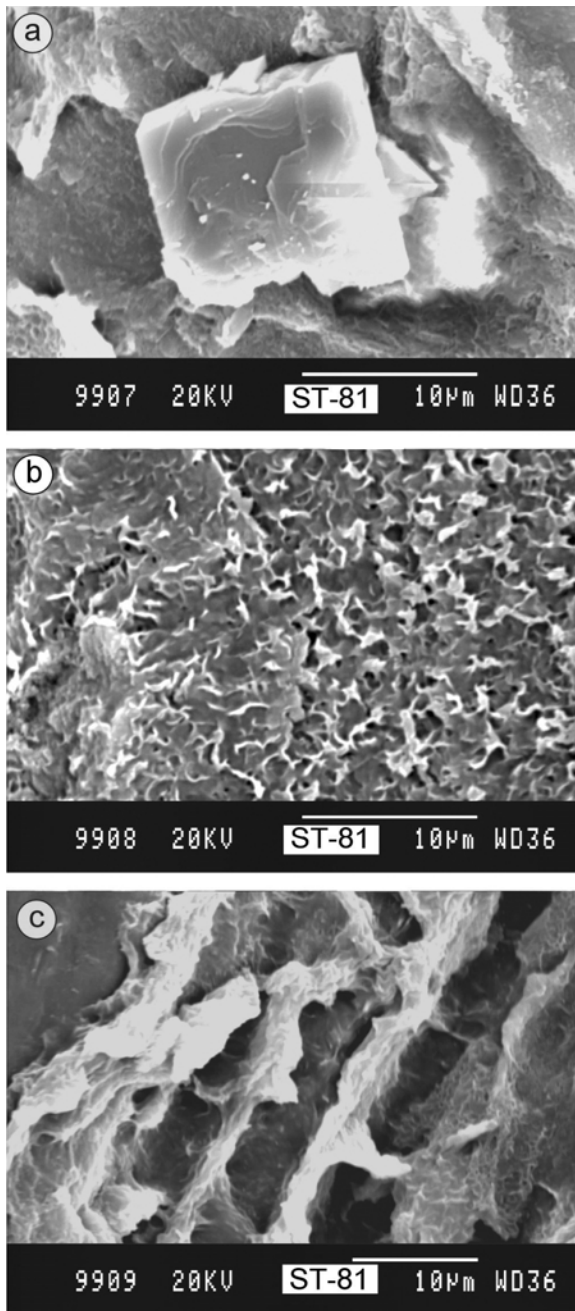
Figure 7. SEM images of sedimentary-hosted talcified serpentinites: (a) rhombohedral dolomite developed within the pores of talcified lizardites; (b) thin and curved talc flakes overgrown on the surface of the matrix; (c) lizardite fibers on the rims of meshes and talc flakes on the surface of the matrix.

The Sivas talc has near end-member compositions with little Al (0.01−0.08) and Fe (0.03−0.13) in tetrahedral sites, as is typical for most talc. The majority of the octahedral positions are filled by Mg (2.68−3.00) and the remainder contains predominantly Fe (0.00−0.21). A negligible amount of Ni (0.01) is present

in the octahedral sheet. Interlayer cations are Mg and Ca with small substitutions of 0.03−0.07 and 0.00−0.04, respectively. An average structural formula of the Sivas talc is as follows:

$$Mg_{0.05}Ca_{0.02}(Mg_{2.91}Fe_{0.05})Si_{3.87}Al_{0.05}Fe_{0.08}O_{10}(OH)_2$$
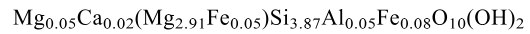
The main tetrahedral cation, Si, is replaced by minor Fe and a negligible proportion of Al in the serpentines. Serpentine is characterized by an extremely high Mg content. The principal substitution occurs very clearly in the octahedral sheet, in which Mg and Fe isomorphously replace one another. The limited substitution of the relatively small amounts of Al, Cr and Ni is also detected in the octahedral sites. The number of total octahedral cations and octahedral charges per formula unit is 2.77−2.91 and 0.01−0.03, respectively. Interlayer cations Mg and Ca are 0.03−0.07 and 0.00−0.01 a.p.f.u., respectively. The unit-cell composition of serpentine corresponds to Fe-lizardite according to the description of Wicks and O'Hanley (1988):

$$Mg_{0.03}Ca_{0.01}(Mg_{2.52}Fe_{0.27}Al_{0.03}Cr_{0.01}Ni_{0.01})$$
$$Si_{1.93}Al_{0.03}Fe_{0.04}O_5(OH)_4$$
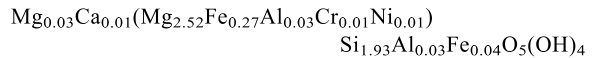
Chemical balance during transformation of serpentine to talc is presented in Figure 11. SiO_2 and P_2O_5 are enriched in the talc composition by a mean of 1.6 and 1.4 times, respectively. In other words, Si and P released from structure of serpentine are used completely in the synthesis of talc. TiO_2, Al_2O_3, Fe_2O_3, MnO, MgO, CaO and Na_2O are depleted in the structure of talc whereas K_2O is both enriched and depleted depending upon the presence or absence of illite layers. The K_2O content of pure talc ranges from 0.00 to 0.18% and does not yield a typical talc composition. This inconsistency can be attributed to the presence of domains (Vali *et al.*, 1993) and/or disordering (Plançon, 2001) with compositional differences in the talc structure as determined in clay mineral structures. MgO and CaO remaining after talcification contribute to the formation of dolomite and/or calcite. Loss of Fe_2O_3 and MnO during conversion to talc seems to have led to the occurrence of Fe- and/or FeMn oxides.

The most notable feature in Figure 11 is the increased fixation of Pb, Bi, In, Mo, As, Ag, Rb, Cs, Ga and Y. Notably, losses of Cr, Ni, Co, Sc and V from transition metals (TM), W from granitoid elements (GE), and Ta, Th and U from high-field strength elements (HFSEs), gains of Be from halogens, Tl from low-field strength elements (LFSEs) and Hf from HFSEs are also observed. In other words, serpentines are carriers of these elements. Increases and decreases are observed for other trace elements such as Cu and Zn from TMs, Sn from GEs, Sb and Ge from miscellaneous elements (ME), Ba and Sr from LFSEs, Nb and Zr from HFSEs.

Chondrite-normalized trace element patterns of selected talc and serpentine minerals from the Sivas region are shown in Figure 12. Chondrite values were
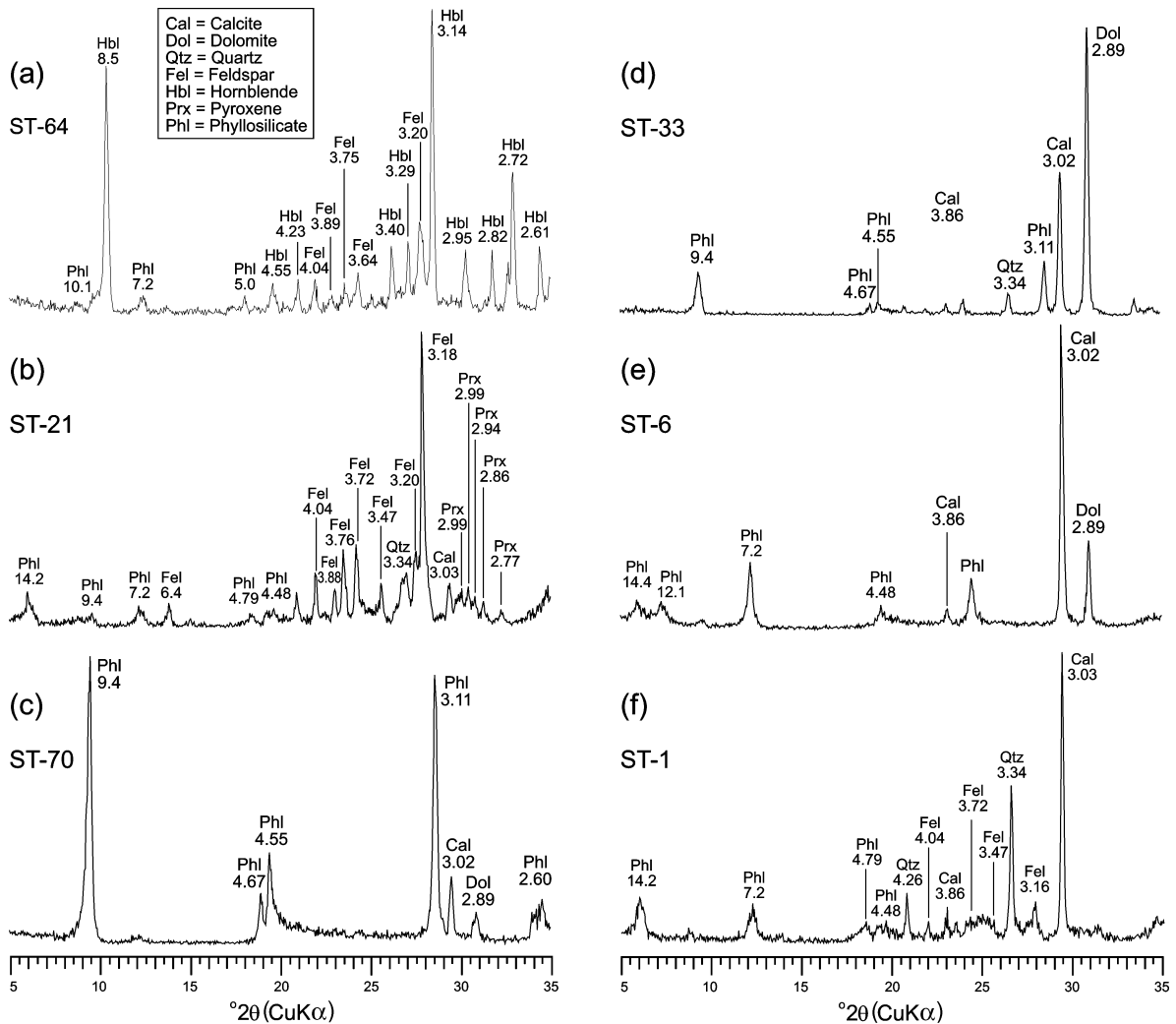
Figure 8. XRD patterns of representative magmatic- and sedimentary-host rocks, (a−c: Yenikervansaray area, d: Yagmurluseki area, e−f: Kurtlukaya area). (a) Uralitic gabbro; (b) altered basalt; (c) talcified serpentinite; (d) dolomitic marl; (e) marl; (f) sandy marl.

obtained from Sun and McDonough (1989). They generally show enrichment in large ion lithophile (LIL) elements relative to HFSEs. The trace element contents of serpentine are greater, except for K, Nb, Sr, Hf and Zr, than those of talc. Serpentine and talc typically have a distinct depletion in P and Ti. In addition to these, serpentine displays clearly positive U and Hf anomalies. As for talc, it has positive Nb and Zr anomalies, and negative Ta and Ce anomalies.

Chondrite-normalized *REE* patterns (Sun and McDonough, 1989) of selected talc and serpentine minerals from the Sivas region are plotted in Figure 13. The *REE* patterns of talc of different origins and serpentine are nearly flat and parallel each other, although the ranges in heavy *REE* concentrations of serpentine with a negative Gd anomaly are greater than those of talc. Light *REE* contents of sedimentary-hosted talc with a negative Gd anomaly are richer than those of the ultramafic-hosted

talc with a negative Eu anomaly as well as serpentine. The *REE* patterns suggest that these minerals were derived and differentiated from the same source.

Stable isotopes

Oxygen and hydrogen isotopic data for one serpentine and three talc samples from the Sivas region are displayed in Table 3. Talc exhibits a narrow range of $\delta^{18}O$ values (+13.8‰ to +17.5‰) and a large range of δD values (-60‰ to -36‰). $\delta^{18}O$ and δD values of talc are different with respect to their host rocks. The isotopic ratio of serpentine plots within and on the edge of the field of Alpine ultramafic types as defined by Wenner and Taylor (1974), whereas those of talc lie along the supergene−hypogene line, with sedimentary-hosted talc close to supergene and ultramafic-hosted talc within the hypogene part (Figure 14). In particular, serpentine and talc from the Sivas region are isotopically
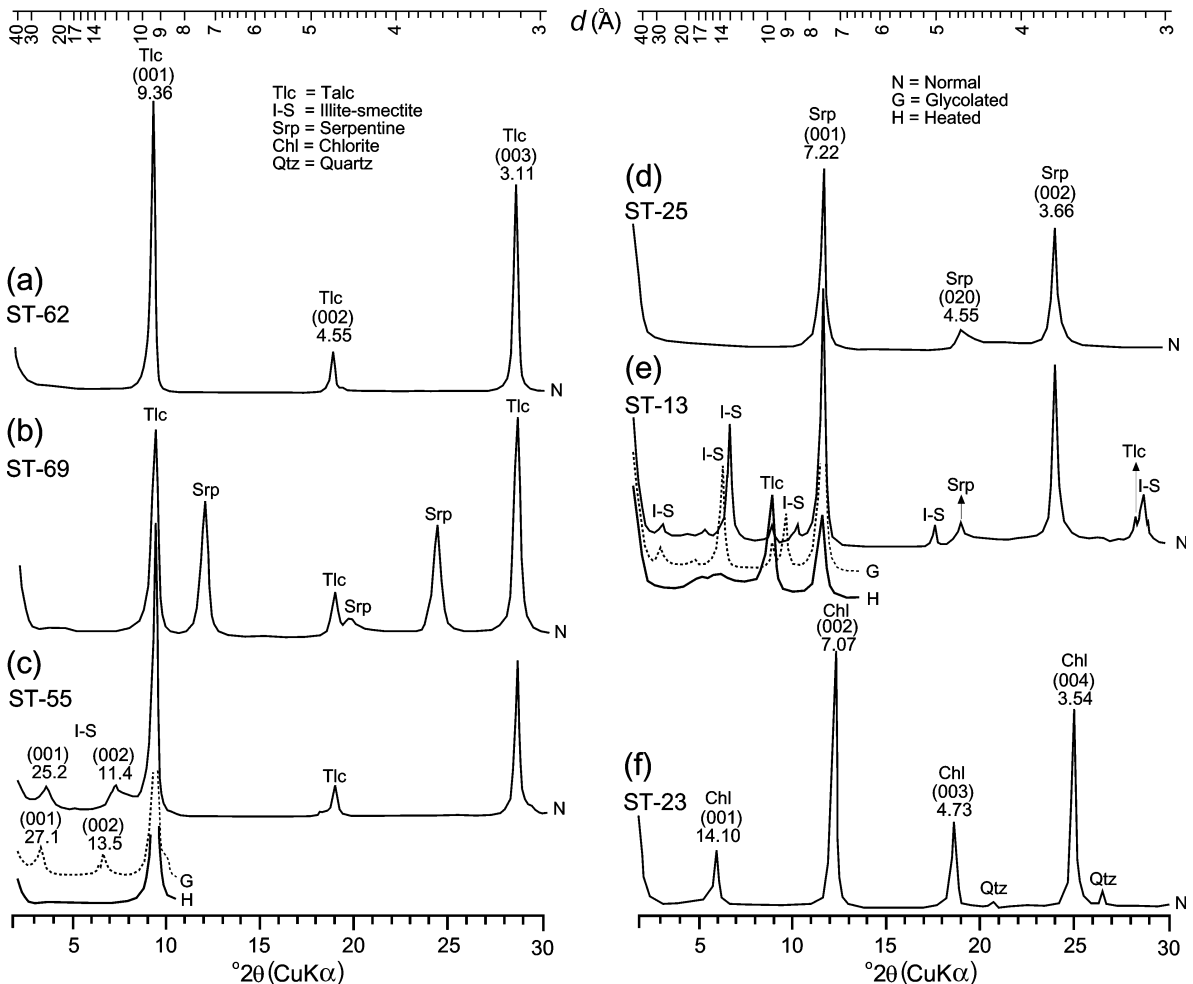
Figure 9. XRD patterns of the <2 μm fraction of representative talc and serpentine assemblages (a−b: Yenikervansaray area, c: Yagmurluseki area, d−f: Kurtlukaya area). (a) Talc in the talcified serpentinites; (b) talc + serpentine in the talcified serpentinites; (c) talc + I-S in the talcified serpentinites; (d) serpentine in the serpentinites; (e) serpentine ± talc ± I-S in the serpentinites; (f) chlorite in the altered volcanics.

distinct from oceanic serpentines and deweylites which are mixtures of serpentine and montmorillonite that form during weathering (Wenner and Taylor, 1974). In addition, it is emphasized that samples from serpentine to ultramafic- and sedimentary-hosted talc have an alteration trend with isotopic fractionation towards diagenetic conditions (Figure 14).

The published estimates of $\delta^{18}O$ for talc-water based on the model of Zheng (1993) agree quite well, as shown in Figure 15, although there are various methods for these mineral pairs (e.g. Savin and Lee, 1988; Zheng, 1993). According to the model of Zheng (1993), the $\delta^{18}O$ data correspond to temperatures of at least 68°C and 80−98°C for the sedimentary- and ultramafic-hosted talc formations, respectively, assuming the talc- and serpentine-forming fluid was seawater ($\delta^{18}O = 0‰$). The formation temperature of sedimentary-hosted talc is somewhat high with respect to marine environments, which suggests that they included the inheritance of ultramafic-hosted talc transported into the basin. As for

serpentinization, it must have occurred at minimum temperatures of 100°C, which is quite similar to those of ultramafic-hosted talc formations.

The sedimentary-hosted talc deposits are clearly diagenetic in origin, which increases the likelihood that circulating meteoric water as well as sea water played a role in their formation. Some assumptions related to oxygen isotopic fractionation vs. temperature for meteoric water could not be made because oxygen isotopic data for starting meteoric fluids have not been documented. Additionally, there are no experimental or theoretical hydrogen isotope fractionation factors for δD/H (talc-water) in the literature (e.g. Brady et al., 1998). For this reason the hydrogen isotopic composition could not be interpreted.

ORIGIN AND FORMATION

In a classic ophiolite sequence (Coleman, 1977), chromite, magnesite and asbestos deposits are associated
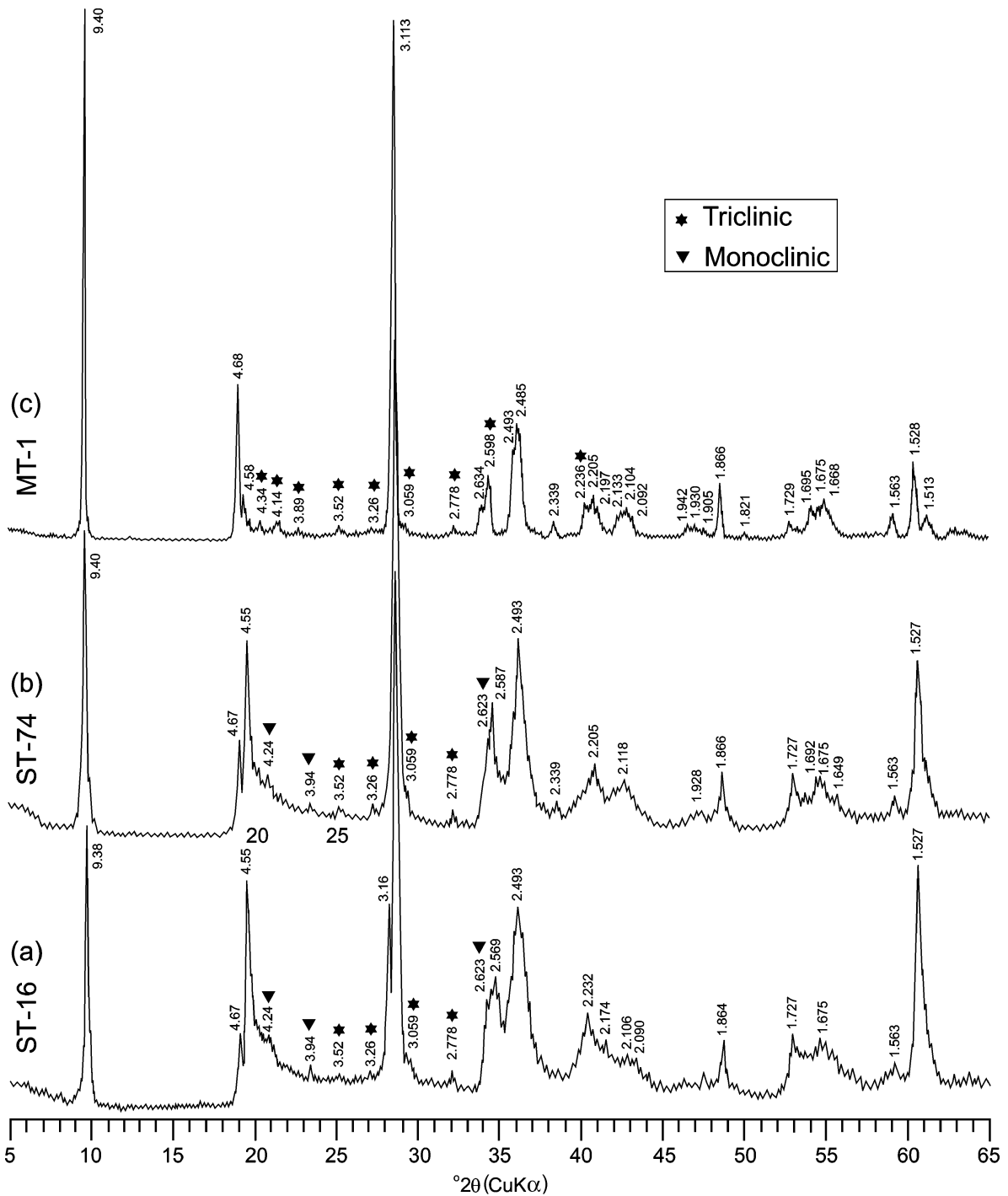
Figure 10. XRD patterns of unoriented powder talc minerals from Turkey (Sivas) and Egypt: (a) sedimentary-hosted talc; (b) ultramafic-hosted talc; (c) Egyptian talc.

with ultramafic rocks as in the Sivas region. Sepiolite occurrences as well as talc, as in this study, are found to occur between cumulates and tectonites (Yalçin and Bozkaya, 2004). However, typical ophicarbonates often associated with talc mineralization are not developed in this zone.

Lizardite derived from olivine occurs at a temperature below 260ºC on the $MgO-SiO_2-H_2O$ equilibrium diagram of Evans and Guggenheim (1988). The mineral assemblages of olivine + enstatite + lizardite in the peridodite and enstatite + hornblende in the gabbro in the Yenikervansaray area indicate that serpentinization

Table 1. Major element analysis (wt.%) and structural formulae of talc and serpentine in the Sivas talc deposits.

Mineral Oxide	Talc					Serpentine	
	ST-8	ST-16	ST-34	ST-74	ST-75	ST-26	ST-29
SiO_2	59.05	59.72	60.46	59.80	59.71	38.16	36.60
TiO_2	0.006	0.001	0.003	0.001	0.006	0.013	0.001
Al_2O_3	0.11	1.10	0.65	1.00	0.16	0.88	1.40
ΣFe_2O_3	3.58	5.11	0.62	2.20	2.43	6.74	10.18
MnO	0.009	0.001	0.010	0.011	0.011	0.090	0.110
Cr_2O_3	0.003	<0.003	<0.003	<0.003	0.280	0.350	0.23
NiO	0.012	0.030	0.054	0.100	0.055	0.232	0.270
MgO	30.44	28.23	31.29	31.60	31.47	38.63	37.47
CaO	0.56	0.16	0.06	0.19	0.37	0.09	0.24
Na_2O	<0.01	<0.01	<0.01	<0.01	0.03	<0.01	<0.01
K_2O	0.13	0.00	0.09	0.00	0.18	0.22	0.00
P_2O_5	<0.01	0.02	0.01	0.02	0.01	<0.01	0.03
LOI	5.48	4.88	5.78	5.01	5.96	15.24	13.42
Total	99.40	99.26	99.04	99.94	100.67	100.67	99.96
Si	3.86	3.88	3.92	3.82	3.86	1.86	1.99
Al	0.01	0.08	0.05	0.08	0.02	0.05	0.01
Fe	0.13	0.04	0.03	0.10	0.12	0.09	0.00
TC	0.14	0.12	0.08	0.18	0.14	0.14	0.01
Al	0.00	0.00	0.00	0.00	0.00	0.00	0.07
Fe	0.04	0.21	0.00	0.01	0.00	0.16	0.37
Cr	0.00	0.00	0.00	0.00	0.01	0.01	0.01
Ni	0.00	0.00	0.00	0.01	0.00	0.01	0.01
Mg	2.94	2.68	3.00	2.97	2.98	2.73	2.31
TOC	2.98	2.89	3.00	2.99	2.99	2.91	2.77
OC	0.00	0.01	0.00	0.01	0.00	0.01	0.03
Mg	0.03	0.05	0.03	0.07	0.05	0.07	0.03
Ca	0.04	0.01	0.00	0.01	0.03	0.00	0.01
ILC	0.14	0.12	0.06	0.16	0.16	0.14	0.02
TLC	0.14	0.14	0.08	0.17	0.14	0.15	0.04

LOI: loss on ignition; TOC: total octahedral cations; OC: octahedral charge; ILC: interlayer charge; TLC: total layer charge.

of dunite and uralitization of gabbro occurred at different temperatures and times, in spite of thermodynamic parameters such as total water pressures, oxygen fugacity, activity of oxides, *etc.*, which can increase or decrease the temperature (*e.g.* Evans and Guggenheim, 1988).

The emplacement mechanism of ophiolites on the continents and also the timing of serpentinization of ultramafic rocks are still debated in the literature (O'Hanley, 1996). Serpentine-related mineralizations are simply divided into three groups (Mittwede, 1996): (1) magmatic or pyrogenetic, *i.e.* pre-serpentinization; (2) syngenetic, *i.e.* directly related to the serpentinization process; and (3) epigenetic, *i.e.* post-serpentinization, covering metamorphism, metasomatism, alteration and weathering. Talc is syngenetic in origin in the ultramafic rocks of the Yenikervansaray area when the formation temperature of talc and serpentine minerals with respect to isotopic data is taken into consideration. There are various subsequent stages in the talc synthesis as well as related neoformation minerals as described in the following reactions (*e.g.* O'Hanley, 1996; Yalçın and Bozkaya, 2004). In talc occurrences, the first stage in the

alteration process is serpentinization of forsterite by hydration:

$$2Mg_2SiO_4 + H_2O + 2H^+ \rightarrow Mg_3Si_2O_5(OH)_4 + Mg^{2+}$$
forsterite   serpentine

The second stage is the hydrolysis of lizardite by means of carbon dioxide or carbonic acid-bearing ground and/or meteoric waters using weak planes such as thrust and shear zones after ophiolite settlement:

$$Mg_3Si_2O_5(OH)_4 + 6H^+ \rightarrow 3Mg^{2+} + 2H_4SiO_4 + H_2O \text{ or}$$
serpentine
$$Mg_3Si_2O_5(OH)_4 + 4H^+ + CO_2 \rightarrow 3Mg^{2+} + 2H_4SiO_4 + CO_3^{2-}$$
serpentine

The third stage is the formation of several carbonate and/or talc associations:

$$2Mg_3Si_2O_5(OH)_4 + 6H^+ \rightarrow$$
$$Mg_3Si_4O_{10}(OH)_2 + 3Mg^{2+} + 6H_2O$$
serpentine   talc
$$Mg_3Si_2O_5(OH)_4 + 4H_2O + CO_2 + Ca^{2+} \rightarrow$$
$$CaCO_3 + 2H_4SiO_4 + 3Mg^{2+} + 4OH^-$$
serpentine   calcite

Table 2. Trace element analysis (ppm) of talc and serpentine in the Sivas talc deposits.

Mineral Element	Talc					Serpentine	
	ST-8	ST-16	ST-34	ST-74	ST-75	ST-26	ST-29
Cr	21	<20	<20	<20	191	2390	1600
Ni	98	217	423	767	432	1820	2090
Co	3	6	52	11	10	103	86
Sc	<1	n.a.	<1	n.a.	<1	11	n.a.
V	<5	<5	9	<5	<5	42	27
Cu	<10	5	137	10	<10	<10	17
Pb	<5	<5	<5	<5	<5	<5	<5
Zn	<30	43	<30	53	77	<30	57
Bi	<0.1	<0.1	<0.1	<0.1	<0.1	<0.1	<0.1
In	<0.1	<0.1	<0.1	<0.1	<0.1	<0.1	<0.1
Sn	4	<1	4	<1	4	4	<1
W	<0.5	0.6	<0.5	0.7	0.6	1.5	1.5
Mo	<2	<2	<2	<2	<2	<2	<2
As	<5	<5	<5	<5	<5	<5	<5
Sb	<0.2	<0.2	<0.2	<0.2	0.3	<0.2	0.3
Ge	0.8	<0.5	1.2	0.8	1.6	0.9	0.6
Be	<1	n.a.	<1	n.a.	<1	<1	n.a.
Ag	<0.5	<0.5	<0.5	<0.5	<0.5	<0.5	<0.5
Rb	<1	<1	<1	<1	<1	<1	<1
Cs	<0.1	0.1	0.1	<0.1	0.1	<0.1	<0.1
Ba	8	<3	<3	5	5	7	3
Sr	16	6	4	2	6	3	4
Tl	<0.05	<0.05	0.07	<0.05	<0.05	0.05	<0.05
Ga	<1	<1	<1	<1	<1	<1	<1
Ta	<0.01	<0.01	<0.01	<0.01	<0.01	<0.01	0.03
Nb	1.7	0.7	0.9	<0.2	0.7	0.4	<0.2
Hf	0.2	0.3	<0.1	0.3	<0.1	<0.1	<0.1
Zr	8	33	2	28	3	<1	5
Y	<0.5	<0.5	<0.5	<0.5	<0.5	<0.5	<0.5
Th	<0.05	0.38	<0.05	0.09	0.06	<0.05	0.92
U	0.03	0.04	0.03	0.02	0.02	0.03	1.05
La	0.08	0.46	0.05	0.10	0.15	<0.05	0.38
Ce	0.17	0.90	0.11	0.12	0.28	0.07	0.72
Pr	0.02	0.10	0.02	0.02	0.03	<0.01	0.08
Nd	0.10	0.36	0.11	0.07	0.17	<0.05	0.36
Sm	0.04	0.04	0.04	0.04	0.04	<0.01	0.06
Eu	0.011	<0.005	0.007	0.005	0.007	<0.005	0.012
Gd	0.02	0.02	0.04	0.03	0.04	<0.01	0.03
Tb	<0.01	<0.01	<0.01	0.01	<0.01	<0.01	<0.01
Dy	0.04	0.03	0.07	0.06	0.05	0.03	0.06
Ho	<0.01	<0.01	0.02	0.01	<0.01	<0.01	0.01
Er	0.02	0.02	0.05	0.04	0.03	0.03	0.05
Tm	<0.005	<0.005	0.008	0.006	<0.005	0.007	0.009
Yb	0.02	0.02	0.05	0.02	0.02	0.06	0.06
Lu	0.003	<0.002	0.009	0.003	0.005	0.010	0.010

Table 3. Isotope ratios of talc and serpentine in the Sivas talc deposits.

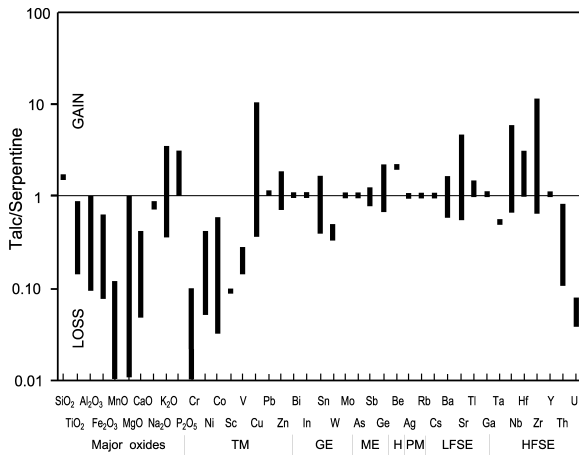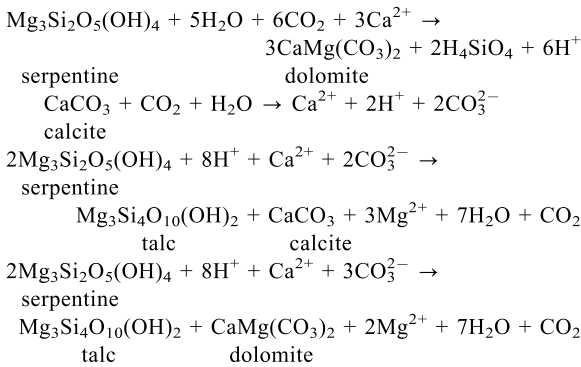| Sample no.	Mineral	Location	Host rock	$\delta^{18}O$‰ (SMOW)	δD‰ (SMOW)
ST-8	Talc	Kurtlukaya	Sedimentary	17.5	−36
ST-34	Talc	Yagmurluseki	Ultramafic	13.8	−60
ST-75	Talc	Yenikervansaray	Ultramafic	15.9	−51
ST-26	Serpentine	Kurtlukaya	Ultramafic	9.4	−88

Figure 11. Chemical variations between talc and serpentine from Sivas talc deposits (TM = transition metal, GE = granitoid element, HFSE = high-field strength element, LFSE = low-field strength element, ME = miscellaneous element).

$$Mg_3Si_2O_5(OH)_4 + 5H_2O + 6CO_2 + 3Ca^{2+} \rightarrow$$

$$3CaMg(CO_3)_2 + 2H_4SiO_4 + 6H^+$$

serpentine   dolomite

$$CaCO_3 + CO_2 + H_2O \rightarrow Ca^{2+} + 2H^+ + 2CO_3^{2-}$$

calcite

$$2Mg_3Si_2O_5(OH)_4 + 8H^+ + Ca^{2+} + 2CO_3^{2-} \rightarrow$$

serpentine

$$Mg_3Si_4O_{10}(OH)_2 + CaCO_3 + 3Mg^{2+} + 7H_2O + CO_2$$

talc   calcite

$$2Mg_3Si_2O_5(OH)_4 + 8H^+ + Ca^{2+} + 3CO_3^{2-} \rightarrow$$

serpentine

$$Mg_3Si_4O_{10}(OH)_2 + CaMg(CO_3)_2 + 2Mg^{2+} + 7H_2O + CO_2$$

talc   dolomite

Opaque minerals, probably magnetite, abundant in some samples, show that Fe released during the serpentinization of fayalitic olivines was probably used to form Fe oxides:

$$4(Mg,Fe)_2SiO_4 + 2H^+ \rightarrow$$

$$Mg_3Si_4O_{10}(OH)_2 + Fe_3O_4 + 2Mg^{2+}$$

Fe-forsterite   talc   magnetite
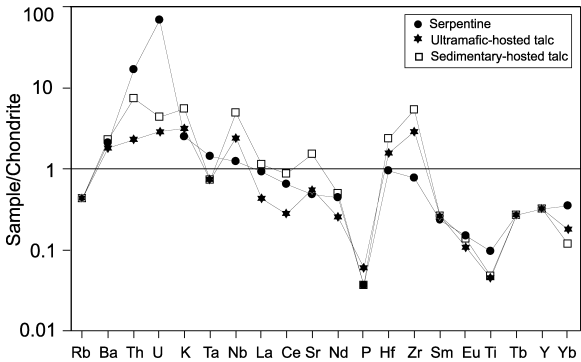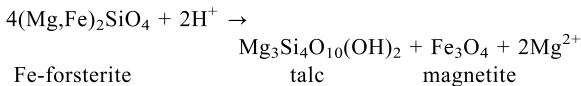
Figure 12. Chondrite-normalized multi-element variation diagram of talc and serpentine minerals from Sivas talc deposits.
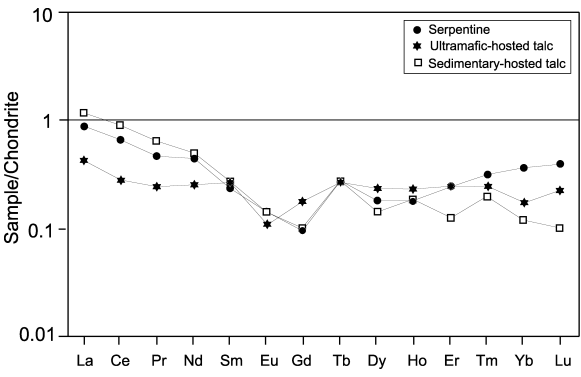
Figure 13. Chondrite-normalized *REE* spider diagram for talc and serpentine from the Sivas talc deposits.

Talc with a sedimentary origin occurs by chemical precipitation based on SEM images which suggest that the source of the large volumes of Mg is serpentinites and talc of the ophiolitic series in the source area. The Mg is transferred into the basin as ions and serpentine and talc phases which were hydrolyzed as formulated below:

$$Mg_3Si_2O_5(OH)_4 + 6H^+ \rightarrow 3Mg^{2+} + 2H_4SiO_4 + H_2O$$

serpentine

$$Mg_3Si_4O_{10}(OH)_2 + 4H_2O + 6H^+ \rightarrow 3Mg^{2+} + 4H_4SiO_4$$

talc

$$Mg_3Si_2O_5(OH)_4 + 2H_4SiO_4 \rightarrow Mg_3Si_4O_{10}(OH)_2 + 5H_2O$$

serpentine   talc
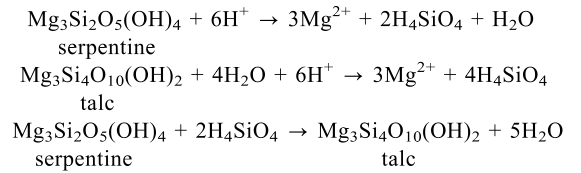
The association of several phyllosilicate and carbonate minerals requires different formation conditions in the sedimentary-hosted talc deposits. Textural relations and mineral paragenesis indicate that carbonates such as calcite and/or dolomite are generally the first minerals to form, whereas phyllosilicates such as talc, smectite, illite, chlorite, C-S and I-S are the last-formed minerals within the marine environment. Clay minerals, except for illite and chlorite with detrital origin, are the products of diagenetic transformation and/or neoformation mechanisms derived from volcanogenic constituents, as emphasized in several localities of the central Anatolian province and other countries (*e.g.* Huff and Türkmenoglu, 1981; Huff *et al.*, 1997; Yalçın, 1997; Yalçın and Gümüşer, 2000).

All data suggest that the formation of both silicates, such as talc, sepiolite and quartz, and carbonates such as calcite, dolomite and magnesite, derived from serpentine, are related to cation and/or oxide ratios in the solution in which $MgO/(MgO+CaO)$ and H_2O/CO_2 are 0.00 and 4.00 for calcite, 0.50 and 0.83 for dolomite, 1.00 and 0.67 for magnesite; and MgO/SiO_2 are 1.50 for serpentine, 0.75 for talc and 0.67 for sepiolite (*e.g.* Yalçın and Bozkaya, 1995, 2004). In other words, occurrences of talc instead of sepiolite are clearly controlled by lesser Mg/H and greater SiO_2 activities (Coleman and Jove, 1992; Birsoy, 2002), and, indirectly,
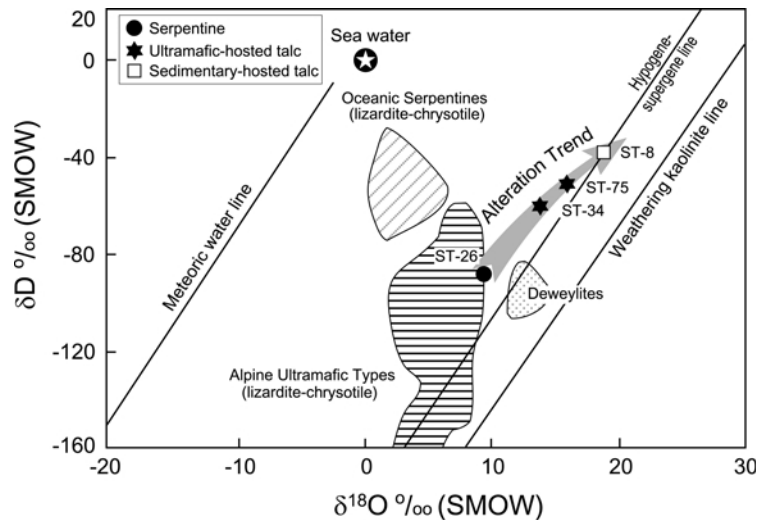
Figure 14. δD-δ^{18}O relations for serpentine and talc isotopic compositions from the Sivas region (Oceanic serpentinites, Alpine ultramafic types and deweylite from Wenner and Taylor, 1974).

the composition of host rocks and lower pH of the environment in the Sivas Basin.

CONCLUSIONS

The detailed features of talc deposits in the Sivas region, Central Anatolia, Turkey, have been determined using field observations, XRD, thin-section and SEM petrography, and major and trace element geochemical considerations. Talc deposits are restricted to the late Cretaceous ophiolitic series and Paleocene units. Talc occurrences related to ultramafic-hosted rocks appear to have a limited economic potential for now, due to a few small outcrops, but the boundary between tectonite and cumulates has yet to be effectively prospected through-

Figure 15. Theoretical oxygen isotopic fractionation between talc and water as a function of temperature as calculated by Zheng (1993).

out the ophiolitic belt. Further new talc occurrences can probably be expected within the Paleocene siliciclastic rocks adjacent to serpentinized ultramafics in the south Anatolian ophiolite belt which commonly provide Mg-rich materials to the basin. However, Mg silicates and carbonates, notably sepiolite-palygorskite and magne-site, were formed within the younger rocks as reported by Yalçin *et al.* (2004).

Talc occurrences from the Sivas region are divided into two groups, as *in situ* alteration products and sedimentary deposits. Of these, the first group was developed between tectonite and cumulate that corre-sponds to a syn-serpentinization stage. The other was found as beds, lenses, nodules and fracture filling within the siliciclastic rocks. The bedded talc is the product of sedimentary precipitation, whereas lens-shaped and nodular talc are diagenetic in origin, and fillings are represented by post-diagenetic neoformation minerals.

The Al, Fe and Mn of the major elements, transition metals except for Pb, Ta, Th and U of the HFSEs, W of granitoid elements, Sb of miscellaneous elements and Er, Tm, Yb and Lu of the *LREE*s were structurally associated with serpentine. In particular, talc of sedi-mentary origin tends to be the principal carrier of Nb, Hf and Zr of the HFSEs and La, Ce, Pr and Nd of the *LREE*s, with respect to serpentine. The ultramafic-hosted talc is enriched in Cr, Ni, Fe, Mg and Co, characteristic of ultramafic rocks and depleted in Ti, P, Zn, V, Ga, Sc, Zr and Sr, characteristic of volcanic rocks. The sedimentary-hosted talc has inherited trace elements and isotopic values from the parent ultramafic rocks and contains no trace elements from the basalts and gabbros from either ophiolitic sequence or hydro-thermal solutions.
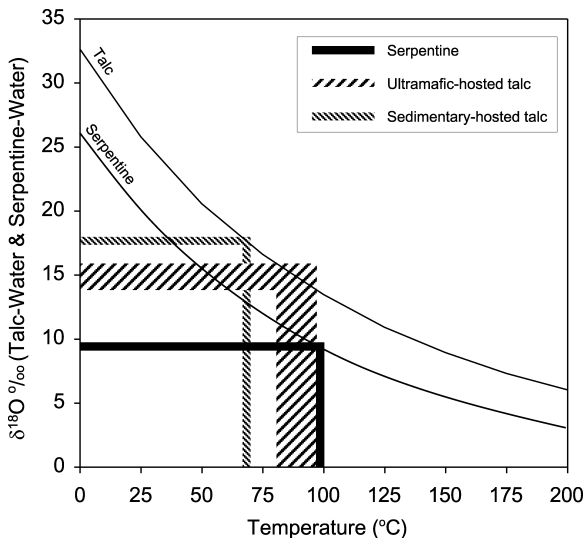
Oxygen and hydrogen isotope data for the talc and serpentine are consistent with 68−98°C and 100°C fluids derived from seawater, based on theoretical models of

the fractionation of oxygen between talc, serpentine and water. The formation temperatures of talc and serpentine are quite similar to each other, suggesting that they occurred during syngenetic subsequent events with increasing $\delta^{18}O$ and δD isotopic fractionation resulting in an alteration trend. The relatively lower temperature of sedimentary-hosted talc suggests supergene conditions in comparison with the hypogene origin of ultramafic-hosted talc and serpentine.

ACKNOWLEDGMENTS

REFERENCES

Aggarwal, P.K. and Nesbitt, B.E. (1984) Geology and geochemistry of the Chu Chua massive sulfide deposit, British Columbia. *Economic Geology*, **79**, 815–825.

Anderson, P.K., Mogk, D.W. and Childs, J.F. (1990) Petrogenesis and timing of talc formation in the Ruby range, southwestern Montana. *Economic Geology*, **85**, 585–600.

Bingöl, E. (1989) *1/2,000,000 scale Turkish Geology Map.* Mineral Research and Exploration of Turkey Publication, Ankara (in Turkish).

Birsoy, R. (2002) Formation of sepiolite-palygorskite and related minerals from solution. *Clays and Clay Minerals*, **50**, 736–745.

Bjerkgard, T. and Bjorlykke, A. (1996) Sulfide deposits in Folldal, southern Trondheim region Caledonides, Norway: Source of metals and wall-rock alterations related to host rocks. *Economic Geology*, **91**, 676–696.

Brady, J.B., Cheney, J.T., Rhodes, A.L., Vasquez, A., Green, C., Duvall, M., Kogut, A., Kaufman, L. and Kovaric, D. (1998) Isotope geochemistry of Proterozoic talc occurrences in Archean marbles of the Ruby Mountains, soutwest Montana, U.S.A. *Geological Materials Research*, **1**, 1–41.

Brindley, G.W. (1980) Quantitative X-ray mineral analysis of clays: Pp. 411–438 in: *Crystal Structures of Clay Minerals and their X-ray Identification* (G.W. Brindley and G. Brown, editors). Monograph **5**, Mineralogical Society, London.

Cater, J.M.L., Hanna, S.S., Ries, A.C. and Turner, P. (1991) Tertiary evolution of the Sivas Basin, Central Turkey. *Tectonophysics*, **195**, 29–46

Coleman, R.G. (1977) *Ophiolites: Ancient Oceanic Lithosphere.* Springer-Verlag, Berlin, 229 pp.

Coleman, R.G. and Jove, C. (1992) Geological origin of serpentinites. Pp. 1–17 in: *The Vegetation of Ultramafic (Serpentine) Soils.* Proceedings of the First International Conference on Serpentine Ecology (A.J.M. Baker, J. Proctor and R.D. Revees, editors), Intercept Ltd., Andover, United Kingdom.

El-Sharkawy, M.F. (2000) Talc mineralization of ultramafic affinity in the Eastern Desert of Egypt. *Mineralium Deposita*, **35**, 346–363.

Evans, B.W. and Guggenheim, S. (1988) Talc, pyrophyllite and related minerals. Pp. 225–294 in: *Hydrous Phyllosilicates (Exclusive of Micas)*, (S.W. Bailey, editor). Reviews in Mineralogy **19**, Mineralogical Society of America, Washington, D.C.

Flanagan, F.J. (1976) Descriptions and analyses of eight new USGS rock standards. Pp. 171–172 in: *Twenty-eight papers present analytical data on new and previously described whole-rock standards* (F.J. Flanagan, editor). United States Geological Survey, Professional Paper, **840**.

Govindaraju, K. (1989) 1989 compilation of working values and sample description for 272 geostandards. *Geostandards Newsletter*, **13**, 1–113.

Gökten, E. (1983) Stratigraphy and geological evolution of the south-southeast of Sarkisla (Sivas). *Bulletin of the Geological Society of Turkey*, **26**, 167–176 (in Turkish, English abstract).

Gökten, E. (1993) Geology of the southern boundary of Sivas basin in the east of Ulas (Sivas-Central Anatolia): tectonic development related to the closure of Inner Tauride Ocean. *Bulletin of the Turkish Association of Petroleum Geologists*, **5**, 35–55 (in Turkish, English abstract).

Görür, N., Tüysüz, O. and Şengör, A.M.C. (1998) Tectonic evolution of the Central Anatolian Basins. *International Geology Review*, **40**, 831–850.

Guezou, J.C., Temiz, H., Poisson, A. and Gürsoy, H. (1996) Tectonics of the Sivas basin: the Neogene record of the Anatolian accretion along the inner Tauric suture. *International Geology Review*, **38**, 901–925.

Hecht, L., Freiberger, R., Gilg, H.A., Grundmann, G. and Kostitsyn, Y.A. (1999) Rare earth element and isotope (C, O, Sr) characteristics of hydrothermal carbonates: genetic implications for dolomite-hosted talc mineralization at Göpfersgrün (Fichtelgebirge, Germany). *Chemical Geology*, **155**, 115–130.

Huff, W.D. and Türkmenoğlu, A.G. (1981) Chemical characteristics and origin of Ordovician K-bentonites along the Cincinnati Arch. *Clays and Clay Minerals*, **29**, 113–123.

Huff, W.D., Bergström, S.M., Kolata, D.R. and Sun, H. (1997) The Lower Silurian Osmundsberg K-bentonite. Part II: Mineralogy, geochemistry, chemostratigraphy and tectono-magmatic significance. *Geological Magazine*, **135**, 15–26.

Huston, D.L., Bolgar, C. and Cozens, G. (1993) A comparison of mineral deposits at the Gecko and White Devil deposits: Implications for ore genesis in the Tennant Creek district, Northern Territory, Australia. *Economic Geology*, **88**, 1198–1225.

Inan, N. and Inan, S. (1990) The features of Gürlevik limestones and a suggested new name of Tecer formation. *Geological Bulletin of Turkey*, **33**, 51–55 (in Turkish, English abstract).

Inan, S., Öztürk, A. and Gürsoy, H. (1993) Stratigraphy of Ulas-Sincan (Sivas) area. *Turkish Journal of Earth Sciences*, **2**, 1–15 (in Turkish, English abstract).

Kavak, K.Ş. (1998) Tectonostratigraphy, tectonic deformation style of Sivas Tertiary Basin around Savcun and Karacaoren (Ulas-Sivas) areas and its study with digital image processing methods. PhD thesis, Cumhuriyet University, Sivas, Turkey, 268 pp. (in Turkish, English abstract).

Koçyigit, A. (1991) An example of an accretionary forearc basin from northern central Anatolia and its implications for the history of subduction of Neo-Tethys in Turkey. *Geological Society of America Bulletin*, **103**, 22–36.

Kurtman, F. (1973) Geological and tectonic structure of Sivas-Hafik-Zara and Imranlı region. *Bulletin of the Mineral Research and Exploration of Turkey*, **80**, 1–32 (in Turkish).

Linder, D.A., Wylie, A.G. and Candela, P.A. (1992)

Mineralogy and origin of the State Line talc deposit, Pennsylvania. *Economic Geology*, **87**, 1607–1615.

Meşhur, M. and Aziz, A. (1980) *Geology and hydrocarbon possibilities of Sivas basin*. Turkish Petroleum Company, Ankara, Report No. **1580**, 28 pp. (in Turkish).

Mittwede, S.K. (1996) Serpentinite-related mineralization. Pp. 144–148 in: *Serpentinites: Records of Tectonic and Petrological History* (D.S. O'Hanley, editor). Oxford Monographs on Geology and Geophysics, **34**. Oxford University Press, Oxford, New York.

Moine, B., Fortuné, J.P., Moreau, P. and Viguier, F. (1989) Comparative mineralogy, geochemistry, and conditions of formation of two metasomatic talc and chlorite deposits: Trimouns, (Pyrenees, France) and Rabenwald (Eastern Alps, Austria). *Economic Geology*, **84**, 1398–1416.

Moore, D.M. and Reynolds, R.C. (1997) *X-ray Diffraction and the Identification and Analysis of Clay Minerals*. Oxford University Press, Oxford, UK, 378 pp.

Naldrett, A.J. (1966) Talc-carbonate alteration of some serpentinized ultramafic rocks, south of Timmins, Ontario. *Journal of Petrology*, **7**, 489–499.

Noack, Y., Decarreau, A. and Manceau, A. (1986) Spectroscopic and oxygen isotopic evidence for low and high temperature origin of talc. *Bulletin de Mineralogie*, **109**, 253–263.

O'Hanley, D.S. (1996) *Serpentinites: Records of Tectonic and Petrological History*. Oxford Monographs on Geology and Geophysics, **34**. Oxford University Press, Oxford, New York, 277 pp.

Önem, Y. (2000) *Industrial Minerals*. Kozan Ltd, Ankara, 386 pp. (in Turkish).

Plançon, A. (2001) Order-disorder in clay mineral structures. *Clay Minerals*, **36**, 1–14.

Poisson, A., Guezou, J.C., Öztürk, A., Inan, S., Temiz, H., Gürsoy, H., Kavak, K.Ş. and Özden, S. (1996) Tectonic setting and evolution of the Sivas Basin, Central Anatolia, Turkey. *International Geology Review*, **38**, 838–853.

Sandrone, R. (1993) Talc deposits in the Italian Western Alps. Pp. 697–700 in: *Geology Applied to Ore Deposits* (P. Fenoll, J. Torres and F. Gevilla, editors). Current Research, Granada.

Savin, S.M. and Lee, W. (1988) Isotopic studies of phyllosilicates. Pp. 189–223 in: *Hydrous Phyllosilicates (Exclusive of Micas)* (S.W. Bailey, editor). Reviews in Mineralogy, **19**, Mineralogical Society of America, Washington, D.C.

Schandl, E.S., Gorton, M.P. and Sharara, N.A. (2002) The origin of major talc deposits in the Eastern Desert of Egypt: Relict fragments of a metamorphosed carbonate horizon? *Journal of African Earth Sciences*, **34**, 259–273.

Sun, S.S. and McDonough, W.E. (1989) Chemical and isotopic systematics of ocean basalts: Implications for mantle composition and processes. Pp. 313–345 in: *Magmatism in Ocean Basalts* (A.D. Saunders and M.J. Norry, editors). Special Publication **42**, Geological Society of London, London.

Şengör, A.M.C. (1979) The North Anatolian fault: its age, offset, and tectonic significance. *Journal of Geological Society of London*, **136**, 268–282.

Şengör, A.M.C. and Yılmaz, Y. (1981) Tethyan evolution of Turkey: A plate tectonic approach. *Tectonophysics*, **75**, 181–241.

Tunç, M., Özçelik, O., Tutkun, Z. and Gökçe, A. (1991) Basic geological characteristics of the Divrigi-Yakuplu-Iliç-Hamo (Sivas) area. *Doğa-Turkish Journal of Engineering and Environmental Sciences*, **15**, 225–245 (in Turkish, English abstract).

Tornos, F. and Spiro, B.F. (2000) The geology and isotope geochemistry of the talc deposits of Puebla de Lillo (Cantabrian Zone, Northern Spain). *Economic Geology*, **95**, 1277–1296.

Vali, H., Martin, R.F., Amarantidis, G. and Morteani, G. (1993) Smectite-group minerals in deep-sea sediments: Monomineralic solid-solution or multiphase mixtures? *American Mineralogist*, **78**, 1217–1229.

Wenner, D.B. and Taylor, H.P. Jr. (1974) D/H and O^{18}/O^{16} studies of serpentinization of ultramafic rocks. *Geochimica et Cosmochimica Acta*, **38**, 1255–1286.

Wicks, F.J. and O'Hanley, D.S. (1988) Serpentine minerals: structures and petrology. Pp. 91–167 in: *Hydrous Phyllosilicates (Exclusive of micas)* (S.W. Bailey, editor). Reviews in Mineralogy, **19**, Mineralogical Society of America, Washington, D.C.

Wicks, F.J. and Plant, G. (1979) Electron microprobe and X-ray microbeam studies of serpentine textures. *The Canadian Mineralogist*, **17**, 785–830.

Wicks, F.J. and Whittaker, E.J.W. (1977) Serpentine textures and serpentinization. *The Canadian Mineralogist*, **15**, 459–488.

Wiewiora, A., Sanchez-Soto, P.J., Avilés, M.A., Justo, A., Pérez-Maqueda, L.A., Pérez-Rodriguez, J.L and Bylina, P. (1997) Talc from Puebla de Lillo, Spain. I. XRD study. *Applied Clay Science*, **12**, 233–245.

Yalçın, H. (1997) Central North Anatolian zeolite occurrences related to Eocene submarine volcanism in Turkey. *Bulletin of Faculty of Engineering Cumhuriyet University Serie A – Earth Sciences*, **14**, 43–56 (in Turkish, English abstract).

Yalçın, H. and Bozkaya, Ö. (1995) Sepiolite-palygorskite from the Hekimhan region (Turkey). *Clays and Clay Minerals*, **43**, 705–717.

Yalçın, H. and Bozkaya, Ö. (2004) Ultramafic-rock-hosted vein sepiolite occurrences in the Ankara ophiolitic mélange, Central Anatolia, Turkey. *Clays and Clay Minerals*, **52**, 227–239.

Yalçın, H. and Gümüşer, G. (2000) Mineralogical and geochemical characteristics of Late Cretaceous bentonite deposits at the north of Kelkit valley, Northern Turkey. *Clay Minerals*, **35**, 807–825.

Yalçın, H. and Inan, N. (1992) Paleontologic, mineralogic and geochemical approaches to Cretaceous-Tertiary transition from Tecer Formation (Sivas). *Geological Bulletin of Turkey*, **35**, 95–102 (in Turkish, English abstract).

Yalçın, H., Gündoğdu, M.N., Gaurgoud, A., Vidal, P. and Uçurum, A. (1998) Geochemical characteristics of Yamadağı volcanics in Central East Anatolia: An example from collision-zone volcanism. *Journal of Volcanology and Geothermal Research*, **85**, 303–326.

Yalçın, H., Bozkaya, Ö. and Başıbüyük, Z. (2004) Mg-mineral occurrences in the Central Anatolian Neogene Intra-cratonic basins related to neotectonic regime: An example from Kangal basin, Sivas, Turkey. *5th International Symposium on Eastern Mediterranean Geology (5th ISEMG)*, Thessaloniki, Greece, pp.1473–1476.

Yılmaz, A. (1983) Basic geology features of the Tokat (Dumanlıdag) and Sivas (Çeltekdagı) areas and the setting of ophiolitic mélange. *Bulletin of Mineral Research and Exploration of Turkey*, **99–100**, 1–18 (in Turkish, English abstract).

Yılmaz, A., Sümengen, M., Terlemez, İ. and Bilgiç, T. (1989) *Geological reconnaissance maps of Turkey: 1:100,000 geological map of the Sivas-G 23 quadrangle*. Mineral Research and Exploration of Turkey Publications, Ankara, 23 pp. (in Turkish).

Zheng, Y.F. (1993) Calculation of oxygen isotope fractionation in hydroxl-bearing silicates. *Earth and Planetary Science Letters*, **120**, 247–263.